Spatio-temporal Dynamics of a Soil Moisture Field: Sampling Error Analysis with Simulation Study

Gwangseob Kim

Kyungpook National University, Faculty of Engineering, Department of Civil Engineering, Taegu, South Korea, 702-701. E-mail: gwangseob@hotmail.com

Abstract- In this study, effects of intermittent visit of observation satellite, partial coverage of remote sensing, heterogeneity of soil properties and precipitation on soil moisture estimations were investigated to develop a sampling strategy. In the soil moisture sampling error analysis, a modified form of theoretical soil moisture model proposed by [1], the WGR model proposed by [2] for use of generating rainfall and the Turning Bands Method for use of generating two dimensional random fields were employed. The evaluation of study results indicates that the sampling error is mainly dominated by sampling interval. The effect of heterogeneity of soil properties and rainfall on sampling error is considerably smaller than that of intermittent visit of observation satellite. The study results suggest that the sampling error generated by other factors such as heterogeneity of rainfall and soil properties, topography and climate conditions can be significantly reduced by increasing the sampling interval, for example, at least twice per day. The effect of partial coverage on sampling error can be ignored provided that the annual mean of coverage portion is higher than 90 %. The impact of water retention capacity of fields on the sampling error seems to be significant. More specifically, the smaller the water retention capacity of fields (i.e., a smaller soil porosity and a thinner active soil depth) the larger the sampling error.

Keywords: Soil moisture estimation, sampling error, remote sensing, the WGR model, the Turning Bands Method.

I. INTRODUCTION

The spatial variability of soil moisture plays an important role in determining spatial characteristics of hydrological processes such as land-atmosphere interactions, rainfall-runoff relationships and soil erosion. In soil moisture estimation studies, lack of available soil moisture data often leads to serious difficulties in selecting the appropriate model type and estimating the model parameters. For a successful soil moisture estimation study, the construction of adequate two-dimensional soil moisture and precipitation data for different soil properties, vegetation, topographic characteristics and climate conditions is required. Recently, characteristics of spatial and temporal variability of soil moisture fields have been studied (e.g. [3, 4] and a number of soil moisture models were proposed in the literature [5, 6, 7, 8]. The influence of soil and rainfall heterogeneities on soil moisture fields was examined in various studies [9, 10, 11].

The following questions still remain for the realization of both spatial and temporal variability of soil moisture fields:

- which soil moisture model(s) can represent both spatial and temporal evolutions of soil moisture appropriately?
- how often should one perform field observations to represent the real soil moisture data structure?
- what is the effect of partial coverage of remote sensing on soil moisture fields?
- how many sensors are needed to represent soil moisture fields? and
- how to decide sensor positions to reduce the sampling error?

In order to find solutions to the above problems, an efficient soil moisture modeling and sensing strategy have to be decided for determining two-dimensional soil moisture fields. The objectives of this study are therefore to analyze the effect of intermittent visit of observation satellite, partial coverage of remote sensing, heterogeneity of soil properties and precipitation on the sampling error and, later, to present an efficient sampling strategy. For this purpose, a modified form of soil moisture model proposed by [1], the WGR model developed by [2] for generating rainfall, and the Turning Bands Method for generating two-dimensional soil porosity, active soil depth and loss coefficient fields were utilized in the model simulations.

II. METHODOLOGY

a) THE SOIL MOISTURE DYNAMICS MODEL

The soil moisture model proposed by [1] is based on the linear reservoir concept, which considers the diffusion effect on soil moisture propagation in space. The original model was modified by the introduction of a stochastic rainfall component as forcing and it is given in the following form:

$$nZ_r \frac{\partial S}{\partial t} = -\eta S + nZ_r(\kappa \nabla^2 S) + D \cdot S \cdot \sin(wt + l) + R \quad (1)$$

where S is relative soil moisture, n is soil porosity, Z_r is depth of surface soil layer, η is loss coefficient, κ is diffusion coefficient, $D\ S\ sin(wt+l)$ is diurnal variation of soil moisture in which D is amplitude of diurnal variation, w is period and l is phase shift, and R is random noise which is replaced with stochastic rainfall model output in this study.

Soil moisture dynamics have the same form of the spatial evolution for crop yield [12]. The balance between soil moisture disturbances caused by the rainfall forcing and the smoothing effects provided by the loss and diffusion terms can be represented by the so called diffusion-injection model which was first considered by [12]. [1] proposed a theoretical soil moisture model with two parameters: the loss and diffusion coefficients. In the model, the loss coefficient represents various processes such as runoff, infiltration and evapotranspiration. The diffusion coefficient is estimated by taking into account both the diffusion through porous media and surface water flow and thus, it takes significantly large values during storm periods and is almost negligible during inter-storm periods. The authors also performed a statistical analysis of the model with the assumption of constant parameters, but both parameters are affected by weather conditions, topography, vegetation and land use. In our study, loss coefficient, soil porosity and active soil depth fields were generated using the Turning Bands Method.

The numerical solution of Eq. (1) was performed employing the Hopscotch method, which can be interpreted as two stage Forward Time Center Space (FTCS) scheme. This scheme is unconditionally stable with a truncation error of $O(\Delta t, \Delta x^2, \Delta y^2)$. Infinite symmetric fields were assumed to treat the boundary conditions. The model equation was discretized in the following forms to be solved at two stages:

First, the following equation was solved at all grid points for which $i+j+k$ is even:

$$\begin{aligned} S_{i,j}^{k+1} &= (1 - \frac{D_{i,j}\sin(wt+l) + \eta_{i,j}}{(nZ_r)_{i,j}}\Delta t - \frac{2\Delta t \kappa_{xi,j}}{\Delta x^2} - \frac{2\Delta t \kappa_{yi,j}}{\Delta y^2})(S_{i,j}^k) \\ &+ (\frac{\Delta t \kappa_{xi,j}}{\Delta x^2})(S_{i+1,j}^k + S_{i-1,j}^k) + (\frac{\Delta t \kappa_{yi,j}}{\Delta y^2})(S_{i,j+1}^k + S_{i,j-1}^k) + \frac{R_{i,j}^k \Delta t}{(nZ_r)_{i,j}} \end{aligned} \quad (2)$$

Later, the following equation was solved at all grid points for which $i+j+k$ is odd:

$$\begin{aligned} S_{i,j}^{k+1} &= (1 - \frac{D_{i,j}\sin(wt+l) + \eta_{i,j}}{(nZ_r)_{i,j}}\Delta t)(S_{i,j}^k)/SUB \\ &+ (\frac{\Delta t \kappa_{xi,j}}{\Delta x^2})(S_{i+1,j}^{k+1} + S_{i-1,j}^{k+1})/SUB \\ &+ (\frac{\Delta t \kappa_{yi,j}}{\Delta y^2})(S_{i,j+1}^{k+1} + S_{i,j-1}^{k+1})/SUB \\ &+ \frac{R_{i,j}^k \Delta t}{(nZ_r)_{i,j}}/SUB \end{aligned} \quad (3)$$

where $SUB = (1 + \frac{2\kappa_{xi,j}\Delta t}{\Delta x^2} + \frac{2\kappa_{yi,j}\Delta t}{\Delta y^2})$

b) THE WGR MODEL

As a conceptual model the WGR model was developed to represent mesoscale precipitation. Incorporating various observed features of rainfall at that scale, the model develops strong links between atmospheric dynamics and statistical descriptions of mesoscale precipitation. As a space-time representation of the rainfall, this particular model is characterized by the arrival mechanism of storm events through time. The model represents rainfall in a hierarchical approach with rain cells embedded in cluster potential centers, which, in turn, are embedded in rain bands. The Poisson process and the spatial Poisson process were introduced for the rain bands arrival scheme and to distribute the cluster potentials within a rain band, respectively. The occurrences of rain cells within the cluster potentials and the rain bands are assumed to be random, independently and identically distributed in the space-time cylinder with a common probability density function.

The representation of the ground level rainfall intensity derived by [2] is given as follows:

$$\Phi(t,x) = \int_{-\infty}^{t} g_1(t-s) Z[s, x - v(t-s)] ds \quad (4)$$

in which v is a uniform and steady drift velocity vector and $Z(t, x)$ is defined by

$$Z(t,x) = \int_{R^2} g_2(s-y) X(t,y) dy \quad (5)$$

[2] assumed g_1 and g_2 to be deterministic and of the form

$$\begin{aligned} g_1(t) &= \exp[-\alpha t]; \quad t \geq 0 \\ g_1(t) &= 0; \quad t < 0 \\ g_2(r) &= \exp[-\frac{r^2}{2D^2}] \end{aligned} \quad (6)$$

where α^{-1} is a quantitative measure of the mean life time and D^2 represents the spatial extent of a rain cell.

The two-stage point cluster field $X(t, y)$, a random field, governs the instantaneous generation of rain cells in time and space, and the kernel $g_2(r)$ distributes the rainfall intensity in space around each cell. The kernel $g_1(t)$ represents the temporal evolution of the life cycle of a rain cell.

The parameters of the WGR model represent the physical features in a mesoscale precipitation event and can also represent spatially elongated precipitation fields, which are observed characteristic of rainfall fields. Although the model can create a good stochastic representation of rainfall events in space and time, it has a complex framework requiring the estimation of a number of parameters. [13, 14, 15] estimated the parameters for different fields through non-linear optimization techniques which minimize the sum of square errors. Due to the large number of parameters and the high non-linearity, estimation itself has been a difficult task. In this study, the model parameters were estimated using Oklahoma Mesonet data during the SGP'97 experiment. The model parameters used to generate rainfall field were listed in the following table.

Table: Description of the WGR model parameters (top panel). The estimates of the WGR model parameter from June to August 1997 on the selected sites of the SGP '97 experimental region (a) and the estimates of the WGR model parameter over winter season on the Brazos Valley, Texas (b).

Parameter	Definition	Units	Range
D	Rainfall intensity spatial attenuation parameter.	km	1.0-5.0
σ	Cell location	km	-
u	Rain band speed relative to ground	km/hr	30
ρ	Mean density of cluster potential	cluster/km	0.01-0.001
ν	Mean number of cells per cluster	-	2.0-8.0
β	Cellular birth rate	1/hr	0.06-6.0
α	Mean cell age	1/hr	0.6-6.0
λ	Mean rain band	1/hr	0.0006-0.06

Parameter	λ((storms/hr)	ρ (CPCs/km2)	ν (cells/CPC)	α (1/hour)	β (cells/hour)	i(mm/hr)	SSQ
			El Reno (SGP'97)				
(a)	0.0153	0.0055	6.5	4.9	0.7886	71.8	0.0429
			Wheelock				
(b)	0.0078	0.0034	5.10	2.04	0.3840	60.0	0.0100

[15]

c) THE TURNING BANDS METHOD

Multidimensional random fields were generated using the Turning Bands Method (TBM) in which uni-dimensional line processes are initially generated in space [16]. Each point in the region R is then assigned a weighted sum of values of the line processes. In this method, the mean, m, the variance, s^2 and the spatial covariance function $C(x_1, x_2)$ of the parameter to be generated are pre-specified and second order stationarity is assumed in this process [17], that is: a) the mean is independent of the position in space;

$$E[Z(x)] = m(x) = m, \quad \forall x \in R^n \tag{7}$$

and b) the covariance function $C(x_1, x_2)$ is dependent on the vector difference (i.e., $s=x_1-x_2$) and not on any particular vector of each point;

$$C(x_1, x_2) = C(x_1 - x_2) = C(s) \tag{8}$$

Given that R^n is n dimensional space and P is the region in which a two- or three- dimensional field is desired to be simulated, lines are generated at any origin, O, in R^n. These lines are generated such that the corresponding direction unit vectors, u, are uniformly distributed on a unit circle or sphere depending on whether a two- or three- dimensional field is generated. Along each line, a second order stationary uni-dimensional process is generated with zero mean and covariance function $C_1(\xi)$ in which ξ is the coordinate on line i. The points in the region of P where values are to be generated, are projected orthogonally onto the line i and the corresponding values of the one-dimensional discrete process are assigned. If $Z_i(\xi_{N\,i})$ is the assigned value for any point N in the region of P from the line process and if L lines of simulated value for point N is given by :

$$Z_s(X_N) = \frac{1}{\sqrt{L}} \sum_{i-1}^{L} Z_i(x_N \cdot u_i) \quad (9)$$

where x_N is the location of the point N, u_i is the vector on line i, and $x_N \cdot u_i$ is the projection of the vector x_i onto the line i.

There are several forms of the covariance function such as exponential, exponential spherical, Bessel and Telis [17]. The exponential covariance function selected for this study is given by

$$C(\xi) = \sigma^2 \exp\left\{ -\left\{ \left(\frac{\xi_1}{\lambda_1}\right)^2 + \left(\frac{\xi_2}{\lambda_2}\right)^2 + \left(\frac{\xi_3}{\lambda_3}\right)^2 \right\}^{1/2} \right\} \quad (10)$$

where ξ_1, ξ_2, and ξ_3 are the separation vectors, λ_1, λ_2 and λ_3 are the correlation lengths and σ^2 is the variance of the field.

The fields of porosity, active soil depth and loss coefficients were generated using the TBM and the Southern Great Plains 1997 (SGP'97) experiment field data. The TBM was chosen due to its computational efficiency in generating large fields and, also, its capability to preserve field statistics of mean, covariance and correlation structure. The accuracy of the TBM is dependent on appropriate choice of model parameters.

III. SIMULATION AND SAMPLING STUDY: PARAMETER ESTIMATION AND DATA DESCRIPTION

The current soil moisture model has four parameters: soil porosity, active soil depth, diffusion coefficient and loss coefficient. The basic data to generate the soil porosity were derived from the Washita'92 soil porosity field with 1 km resolution. The field has a mean of 0.443, a standard deviation of 0.034 and a correlation length of 4.48 km.

The loss coefficient field was generated using the ensemble mean and standard deviation of loss coefficients estimated from the Monsoon 90' data which yield different loss coefficients about 10% of soil moisture due to varying metric potentials. A lower loss coefficient was employed for relative soil moisture level under 10%.

The mean value of the active soil depth is 0.5 m as suggested by [1], while the standard deviation and the correlation length are 10% of the mean value and 4.48 km, respectively.

An estimate of the diffusion parameter was obtained using the relationship given by $\kappa = (v^2 t)/4$ for two different hydrologic conditions of storm and inter-storm periods. Here, the typical velocity associated with the front advance is about 20 cm/day and the inter-storm period is about 48 hours. Given that, the lower bound of the diffusion parameter is found 10^{-3} m^2/h. The overland flow velocity is about a few to tens if cm/s and storm duration was assumed to be around 10 hours. Therefore, the upper bound of diffusion parameter is about 10^5 m^2/h [1].

The rainfall fields were generated using the parameters estimated by the WGR from the Oklahoma Mesonet data during the SGP'97 experiment for summer season and from the Brazos Valley of Texas data for winter season (see the table).

The field of study has 100×100 pixels with a 1 km grid dimension in the horizontal and lateral directions. The simulations were performed with a simulation time interval of 1 hour for a simulation period of 1 year. Three different sensing radiuses of 50, 70 and 90 km were utilized for realizing the effect of partial coverage of remote sensing. Each sensing radius has an annual mean of coverage with 48, 74 and 93 %, respectively.

IV. DISCUSSION OF RESULTS AND CONCLUSIONS

A schematic diagram of the simulation study was provided in Fig.1 where the standard procedure was described. The simulation results were depicted in Figs. 2-7 in which each point represents the ensemble mean value of 100-month realizations.

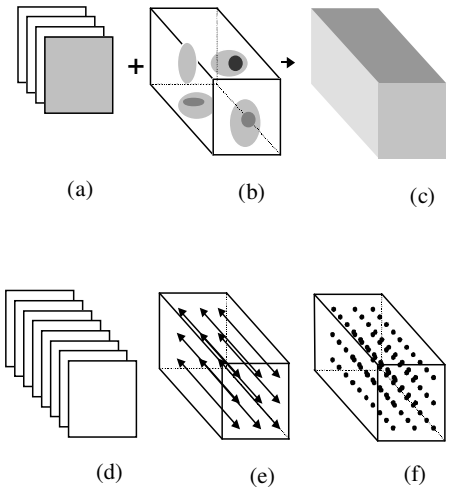

Fig. 1. A schematic diagram of the simulation study: (a) generating several fields of porosity, topology, active soil depth and loss coefficient, (b) generating rainfall field, (c) generating soil moisture field, (d) remotely sensed data from satellite and/or airplane, (e) soil moisture gage design, (f) discrete sampling in space and time.

Fig. 2 indicates the effect of intermittent visit of the observation satellite for two different rainfall fields. Referring to the figure both the sampling error and its standard deviation increase as the sampling interval increases suggesting that the sampling error is dominated by the sampling interval. Also, the sampling error pattern does not change dramatically with the heterogeneity of rainfall associated with the seasonal difference.

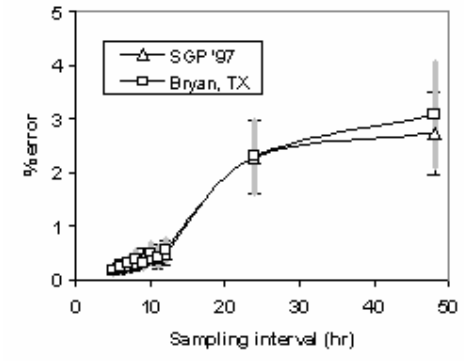

Fig. 2 Sampling error for the intermittent visit of the observation satellite in different rainfall fields.

Fig. 3 shows that the effect of partial coverage on the sampling error is negligible for an annual mean of coverage about 90%. This suggests that although the remote sensing area partially covers the field of analysis the available data are able to reflect the soil moisture properties given that the mean value of coverage portion during the simulation period is greater than 90 %.

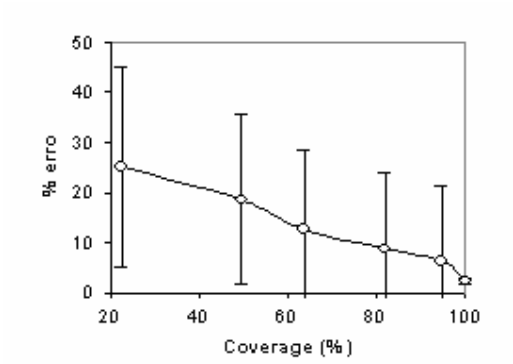

Fig. 3 Sampling error for the partial coverage ranging between 23 and 95 % with daily sampling.

Figs. 4-6 reveal that water retention capacity of fields plays an important role in the sampling error. More specifically, the smaller the water retention capacity (i.e., a smaller soil porosity and active soil depth with a larger loss coefficient) the larger the sampling error.

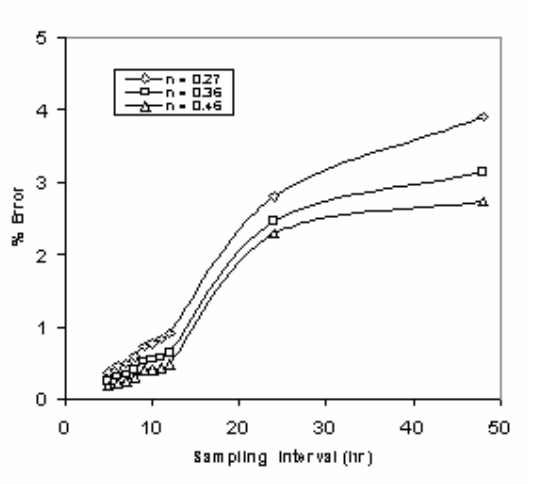

Fig. 4. Sampling error for different porosity fields.

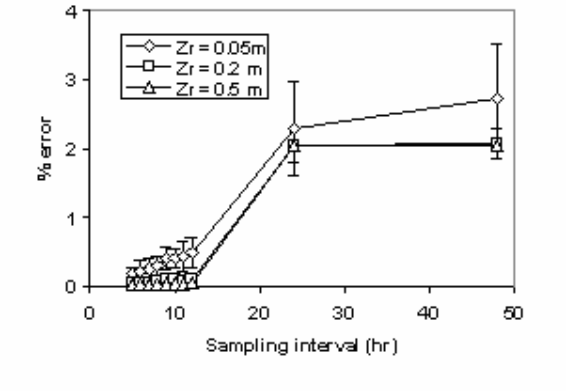

Fig. 5. Sampling error for different active soil depths.

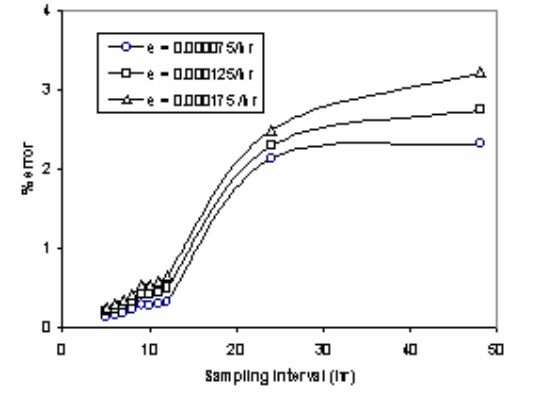

Fig. 6. Sampling error for different loss coefficients.

Finally, Fig. 7 displays that the sampling error of daily sampling increases significantly with the increase of the amplitude of the diurnal cycle.

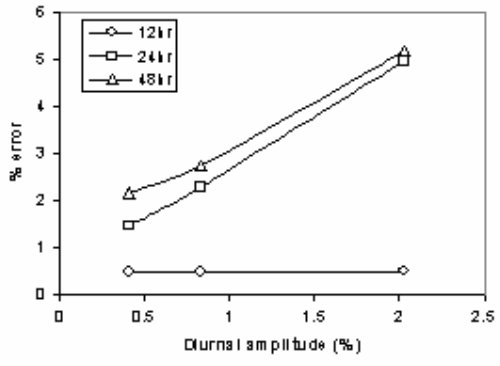

Fig. 7. Sampling error for different amplitude of diurnal impact with the sampling intervals of 12, 24, and 48 hrs, respectively.

Overall, the simulation results suggest that the sampling error is dominated by the sampling interval. In summary, the evaluation of the results shows that:

- the influence of heterogeneity of soil properties and rainfall on the sampling error is smaller than that of the intermittent visit of observation satellite,
- the effect of water retention capacity of fields on the sampling error is significant,
- the impact of partial coverage on the sampling error can be disregarded provided that the annual mean of coverage portion is about 90 %, and
- the sampling error generated by factors such as the heterogeneity of rainfall and soil properties, topography and climate can be dramatically reduced by smaller sampling intervals.

Acknowledgements: This research work was supported by the Korean Ministry of Science & Technology registered as 04-06-08. The authors wish to thank Dr. Osman YILDIZ of Kırıkkale University, Turkey, for his recommendations and corrections on the manuscript.

V. REFERENCES

[1] D. Entekhabi and I. Rodriguez-Iturbe, "Analytical framework for the characterization of the space-time variability of soil moisture". *Advances in Water Resources*, **17**, 25-45, 1994.

[2] E. Waymire, V.K. Gupta and I. Rodriguez-Iturbe, "Spectral theory of rainfall intensity at the Meso-β scale", *Water Resources Research,* **20**(10), 1453-1465, 1984.

[3] D. Entekhabi and P.S. Eagleson, "Land surface hydrology parametrization for atmospheric general circulation models including subgrid scale spatial variability", *J. Climate*, **2**, 816-831, 1989.

[4] G. Kim and A.P. Barros, A.P., "Space-time characterization of soil moisture from passive microwave remotely sensed imagery and ancillary data", *Remote Sensing of Environment*, **81**, 393-403, 2002.

[5] K.L. Brubaker and D. Entekhabi, "An analytic approach to modeling land-atmosphere interaction 1. Construct and equilibrium behavior", *Water Resources Research*, **31**(3), 619-632, 1995.

[6] I. Rodriguez-Iturbe, D. Entekhabi and R.L. Bras, "Non-linear dynamics of soil moisture at climate scales 1. Stochastic analysis", *Water Resources Research*, **27**(8) 1899-1906, 1991a.

[7] I. Rodriguez-Iturbe, D. Entekhabi, J.S. Lee and R.L. Bras,"Non-linear dynamics of soil moisture at climate scales 2. Chaotic analysis", *Water Resources Research*, **27**(8), 1907-1915, 1991b.

[8] P.S. Eagleson, "Climate, soil and vegetation 3. A simplified model for soil moisture movement in the liquid phase", *Water Resources Research*, **14**(5), 722-730, 1978.

[9] C.P. Kim and J.N.M. Stricker, "Influence of spatially variable soil hydraulic properties and rainfall intensity on the water budget", *Water Resources Research*, **32**(6), 1699-1712, 1996.

[10] C.E. Graves, J.B. Valdés, S.S.P. Shen and G.R. North, "Evaluation of sampling error of precipitation from space and ground sensors", *Journal of Applied Meteorology*, **32**, 374-384, 1993.

[11] G.A. Meehl and W.M. Washington, "A comparison of soil moisture sensitivity in two climate models", *Journal of Atmospheric Science*, **45**, 1476-1492, 1988.

[12] P. Whittle, "Topographic correlation, power-law covariance functions, and diffusion", *Biometrica*, **49**(3), 305-314, 1962.

[13] S. Islam, R.L. Bras and I. Rodriguez-Iturbe," Multi-dimensional modeling of cumulative rainfall: parameter estimation and model adequacy through a continuum of scales", *Water Resources Research*, **24**, 992-995, 1988.

[14] J.B. Valdés, S. Nakamoto, S.S.P. Shen and G.R. North, "Estimation of multi-dimensional precipitation parameters by Arial estimates of oceanic rainfall", *Journal of Geophysical Research (Atmos.)*, **95**(D3), 2101-2111, 1990.

[15] R.W. Keopsell and J.B. Valdés, "Multi-dimensional rainfall parameter estimation from sparse network", *ASCE Journal of Hydraulic Engineering*, **117**, 832-850, 1991.

[16] G. Matheron, "Intrinsic random functions and their applications", *Advances in Applied Probability*, **5**, 439-448, 1973.

[17] A. Mantoglou and J.L. Wilson, "The turning bands method for simulation of random fields using line generation by a spectral method", *Water Resources Research,* **18**(5), 1379-1394, 1982.